

1 Parametric design and multi-objective optimisation of containerships

2

3 Alexandros PRIFTIS<sup>a</sup>, Evangelos BOULOUGOURIS<sup>b</sup>, Osman TURAN<sup>a</sup> & Apostolos

4 PAPANIKOLAOU<sup>c</sup>

5 <sup>a</sup>University of Strathclyde, Glasgow, United Kingdom

6 <sup>b</sup>Maritime Safety Research Centre, University of Strathclyde, Glasgow, United Kingdom

7 <sup>c</sup>Hamburgische Schiffbau Versuchsanstalt GmbH, Hamburg, Germany

8

9 **ABSTRACT:** The fluctuation of fuel price levels along with the continuous endeavour of the shipping  
10 industry for economic growth has led the shipbuilding industry to explore new designs for various  
11 types of ships. In addition, the introduction of new regulations by the International Maritime  
12 Organisation frequently triggers changes in the ship design process. In this respect, proper use of  
13 computer-aided ship design systems extends the design space, while generating competitive solutions  
14 in short lead time. This paper focuses on multi-objective optimisation of the design of containerships.  
15 The developed methodology is implemented on CAESES® software and is demonstrated by the  
16 conceptual design and optimisation of a 6,500 TEU containership. The methodology includes a  
17 parametric model of the ship's external and internal geometry and the development and calculation of  
18 all required properties for compliance with the design constraints and verification of the key  
19 performance indicators. The latter constitute the objective functions of the multi-objective  
20 optimisation problem. The energy efficiency design index, the ratio of the above to below deck  
21 number of containers, the required freight rate, the ship's zero-ballast container capacity and the total  
22 ship resistance were used in this study. Genetic algorithms were used for the solution of this multi-  
23 objective optimisation problem.

24

25 **KEYWORDS:** parametric; design; holistic; multi-objective; optimization; containership

26

27 1 INTRODUCTION

28

29 1.1 Container shipping industry

30

31 Global containerised trade has been on constant growth since 1996. It is worth mentioning that in  
32 2015, there was a 2.4% growth, which can be translated to a total movement of 175 million TEUs in  
33 one year (UNCTAD, 2016). The fluctuation of fuel price has caused changes in the operation of ships.  
34 Since 2008, the fuel price has dropped and nowadays heavy fuel oil (HFO) costs as low as 250 \$/t.  
35 Marine diesel oil (MDO) has been following similar course and can be found at prices of around 450  
36 \$/t (Ship & Bunker, 2017). However, this does not always result in lower shipping rates. The  
37 introduction of emission control areas (ECAs) has affected the fuel type ships use. Use of low sulphur  
38 fuel is now required in certain parts of the world. The price difference between fuel types can be  
39 significant. In addition, the recent landmark decision by the International Maritime Organisation  
40 (IMO) Marine Environment Protection Committee to implement a global sulphur cap of 0.5% m/m  
41 (mass/mass) from 1 January 2020 has introduced a step change to the framework of designing and  
42 operating ships (IMO, 2016).

43

44 In the years before 2014 and the collapse of the fuel prices, the shipping industry was adopting several  
45 practices to reduce fuel consumption. One of them was slow steaming (SS) (Tozer, 2008) and super  
46 slow steaming (SSS) (Maloni et al., 2013, Bonney & Leach, 2010). In comparison to some years ago -  
47 when operational speeds of around 25 knots were common- containerships nowadays travel at around  
48 18-20 knots in slow steaming and at 15 knots in super slow steaming. Ship design for lower speeds  
49 has major impact to fuel savings and may reduce their energy efficiency design index (EEDI) levels  
50 (White, 2010).

51

52 The recent improvements in technology and engineering have made the introduction of ultra large  
53 container vessels possible. A new trend, known as cascading, resulted from the high number of new  
54 building programmes initiated by many liner companies. These orders consisted primarily of very  
55 large containerships. The continued influx of such large vessels into the market has led to a large  
56 number of vessels being cascaded onto trade lines that historically have been served by smaller

57 vessels (Köpke et al., 2014). Hence, routes where 2,000-3,000 TEU containerships are preferred by  
58 charterers at the moment may attract larger vessels in the near future. Since the former category of  
59 ships is mainly used for the purpose of short sea shipping, ships in the 6,000 TEU category could  
60 become widely popular among the ship owners and the charterers. In addition, the recent opening of  
61 the new Panama Canal locks means that the Post-Panamax containerships can be utilised in more  
62 transport routes, including the trans-Panama services (van Marle, 2016).

63

64 Although container carriers do not spend considerable amount of time in ports, port efficiency is  
65 considered as one of the most important factors in containership design. The less port time they spent,  
66 the more time is available for cruising at sea, which means that vessels can operate in lower speeds  
67 and consequently reduce fuel consumption. Usually, the transport efficiency is optimised by focusing  
68 on the schedule of the ships visiting a specific port (Kurt et al., 2015). However, in our case the  
69 optimisation focuses on the ship itself, making the incorporation of the port efficiency in the holistic  
70 optimisation of containerships possible. In this study a simplified approach was used, namely  
71 monitoring the ratio of the above to below deck containers' number. As Soutanias (Soutanias, 2014)  
72 has found, the larger the ratio, the faster the loading and unloading of containers; thus, the time spent  
73 by ships in port is reduced.

74

## 75 1.2 International regulatory framework

76

77 Recent developments in the international maritime regulations are going to greatly affect future ship  
78 designs and particularly containerships. One major development is the introduction of the EEDI, in  
79 2012 (IMO, 2012a, c, b). This is a major step forward in implementing energy efficiency regulations  
80 for ships, limiting greenhouse gas emissions, through the introduction of the EEDI limits for various  
81 ship types. The EEDI relates the CO<sub>2</sub> emissions of a ship to her transportation work and is in fact an  
82 indicator of a vessel's energy efficiency. The determination of EEDI is based on a rather complicated  
83 looking (but indeed simple) formula, while it is required that the calculated value is below a reference  
84 line set by the IMO regulation for the specific ship type and size. The EEDI requirement for new ships

85 started with some baseline values in 2013, and is being lowered (thus becoming more stringent)  
86 successively in three steps until 2025, when the 2013 baseline values will have been reduced by 30%.  
87 It is evident that EEDI is a ship efficiency performance indicator that should be minimised in the  
88 frame of a ship design optimisation.

89

90 New rules have been recently developed regarding the control and management of ships' ballast water  
91 and sediments and will be applied to all ships as of September 2017 (IMO, 2004). Although various  
92 systems and technologies aiming at the minimisation of the transfer of organisms through ballast  
93 water to different ecosystems are currently available, their installation on board ships increases their  
94 capital and operating costs. Therefore, research has been focusing lately at solutions to reduce the  
95 amount of required ballast water. This problem is more severe for containerships, which inherently  
96 carry more ballast water, even at the design load condition, for which the ratio of the containers  
97 carried on deck to those carried under deck should be maximised. Thus, design solutions for modern  
98 containerships that consider zero or minimal water ballast capacities are very appealing to the ship  
99 owners. Nevertheless, attention should be paid to the overall cargo capacity as well, so as to maintain  
100 competitive values in all respects.

101

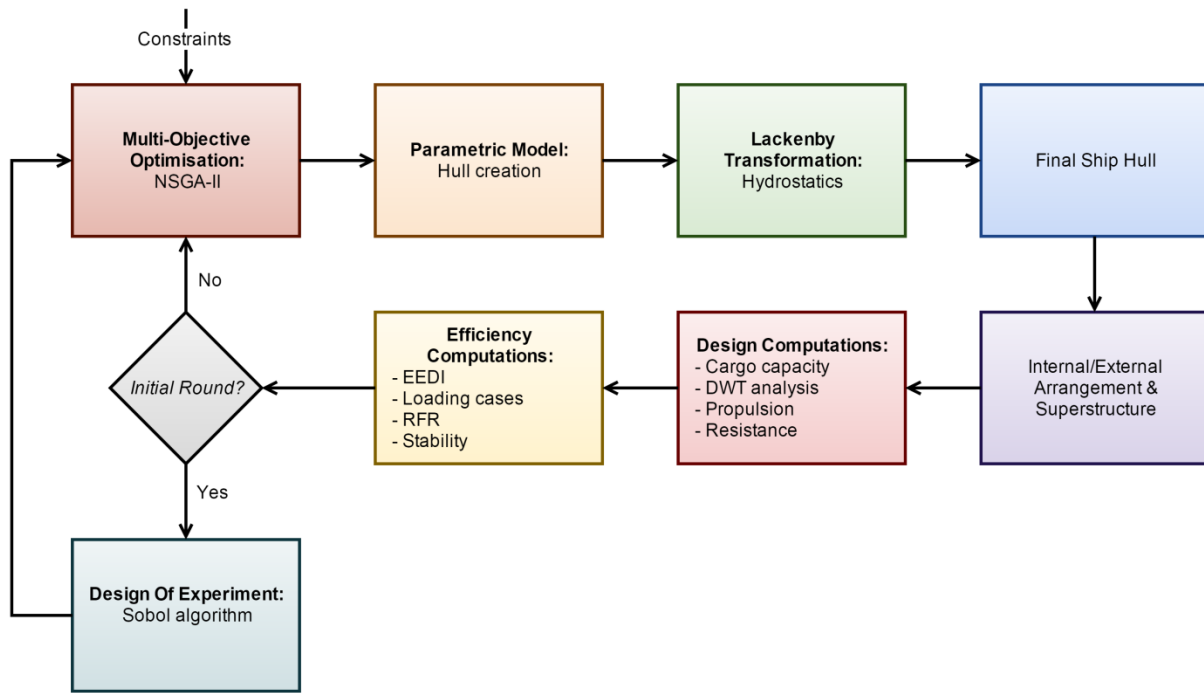
102 Finally, as far as safety regulations are concerned, a new generation of intact stability criteria is  
103 currently being developed by the IMO (IMO, 2015). The introduction of ships with newly developed  
104 characteristic and operation modes has challenged the assumption that the current criteria are  
105 sufficient to prove their stability. Hence, the new criteria will be performance-based and will address  
106 five modes of stability failure; parametric roll, pure loss of stability, excessive acceleration, stability  
107 under dead ship condition and surf-riding/broaching (Peters et al., 2011). As far as containerships are  
108 concerned, parametric roll is considered to be one of the most important modes of stability failure  
109 (Spyrou, 2005). Hence, the draft criteria of level 1 and 2 for parametric roll failure mode according to  
110 SDC 2/WP.4 (IMO, 2015) are applied as part of the optimisation process in this study.

111

113

114 In recent years, several researchers have presented significant computer-aided design (CAD)  
115 methodologies dealing with ship design process and inherently its optimisation (Brown & Salcedo,  
116 2003, Campana et al., 2009, Mizine & Wintersteen, 2010). A common characteristic of most of the  
117 earlier presented works is that they are dealing with specific aspects of ship design or with new  
118 system approaches to the design process. On the other hand, the present study deals with a fast,  
119 holistic optimisation of a Post-Panamax, 6,500 TEU containership, focusing on optimisation of the  
120 ship's arrangements, while considering all side effects on ship design, operation and economy (Priftis,  
121 2015). Holism is interpreted as a multi-objective optimisation of ship design and is based on the main  
122 idea that a system, along with its properties, should be viewed and optimised as a whole and not as a  
123 collection of parts (Papanikolaou, 2010). Efforts are currently being made in the framework of the  
124 European Union funded HOLISHIP project, in that respect (HOLISHIP, 2016). According to the  
125 project's approach, a proposed model follows modern computer-aided engineering (CAE) procedures  
126 and integrates techno-economic databases, calculation and optimisation modules and software tools  
127 along with a complete virtual model which allows the virtual testing before the building phase of a  
128 new vessel. Within this context, a parametric ship model of ship's external and internal geometry is  
129 created at first, followed by a multi-objective optimisation to determine an optimal design (Fig. 1).

130



131

132 Figure 1: Design optimisation procedure

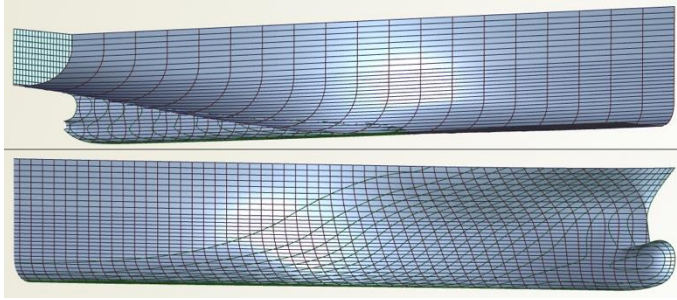
133

134 2.1 Parametric model

135

136 Modern CAD/CAE software tools are used to generate the parametric ship model, following the  
 137 principles of a fully parametric design. The geometric model is produced within CAESES®  
 138 (Friendship Systems, 2017), and consists of four main parts; the main frame, the aft body, the fore  
 139 body, and the main deck (Fig. 2). An initial hull form is used as a baseline for our model and is  
 140 transformed to get the desired hull shape for this study’s baseline model. In order to achieve this,  
 141 several parameters are defined to control certain parts of the hull. Apart from the main dimensions of  
 142 the hull, parameters are introduced to control specific areas at the aft and fore ends. For example, the  
 143 bilge height and width, the shape of the bulbous bow, as well as the position of the propeller tube and  
 144 the transom are controlled by parameters.

145



146

147 Figure 2: Modelled aft and fore body

148

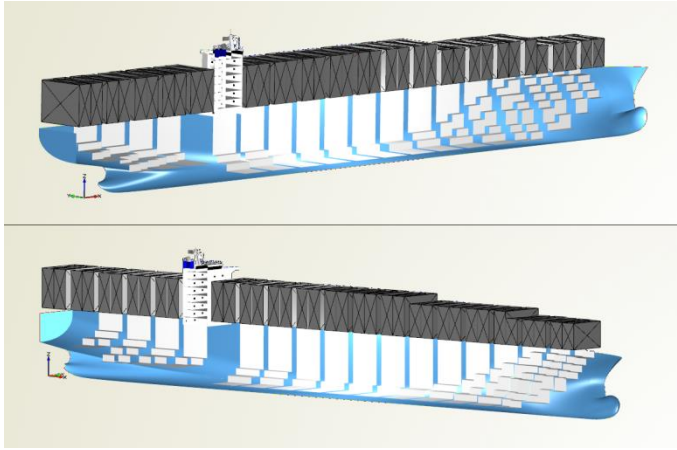
149 In order to create an adequately faired and smooth hull surface, a Lackenby transformation is applied  
150 (Lackenby, 1950). It starts with a hydrostatic and sectional area curve calculation. These are used as  
151 input to the Lackenby transformation. By adjusting the prismatic coefficient ( $C_p$ ) and the longitudinal  
152 centre of buoyancy (LCB), the final hull geometry is produced. This process allows shifting sections  
153 aft and fore, while fairness optimised B-Splines are utilised (Abt & Harries, 2007).

154

155 Next step is to create the superstructure and the cargo arrangements (Figs. 3, 4). New programmes (or  
156 “features”, as they are called within CAESES®) were developed for this purpose. Taking into account  
157 several parameters, such as the number of decks, the bay spacing, the double bottom and double side  
158 distances, the required surfaces are produced to build the deckhouse and the cargo arrangement below  
159 and above the main deck. The feature responsible for the creation of the superstructure takes as input  
160 the number of tiers above the main deck, the desired position along the longitudinal direction, the  
161 height of each deck and the dimensions of the superstructure in the longitudinal and transverse  
162 directions in order to build the superstructure in the appropriate position. The feature responsible for  
163 the development of the internal cargo storage arrangement creates the surface on which the TEUs are  
164 stored, while monitoring the distance of this inner surface from the outer cell of the hull. The feature  
165 responsible for the development of the cargo storage arrangement above the main deck is designed in  
166 such a way, so as to take into account the visibility line rule imposed by the IMO (IMO, 1991). The  
167 feature automatically takes as input the visibility line and the number of deckhouse decks, both of  
168 which are defined in the model. This prevents an excessive vertical stowage of containers above the

169 main deck. In addition, the feature follows the deck line and monitors the available space along the  
170 beam of the ship to define the proper amount of TEU rows above the main deck.

171



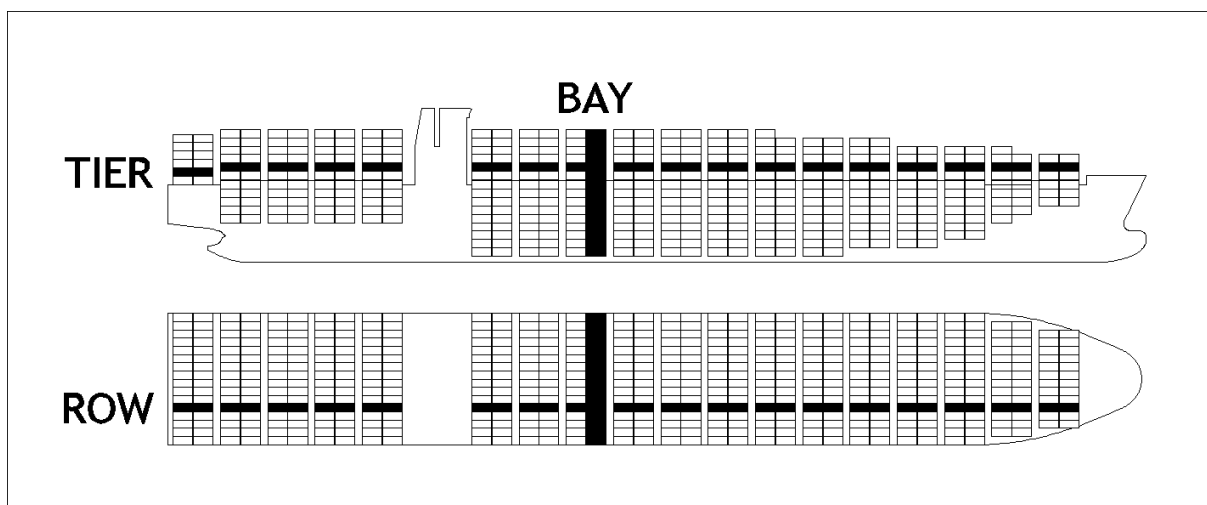
172

173 Figure 3: Parametric model

174

175 In both cases, several parameters are used to define the cargo space, such as the bay spacing and the  
176 dimensions of the standardised TEU unit. The computations are performed separately for each bay, so  
177 that maximum cargo storage capacity is guaranteed by taking advantage of every available space  
178 within the hull, especially in the regions where the complexity of the geometry is higher (e.g. the bow  
179 area).

180



181

182 Figure 4: Definition of bays, rows and tiers in a containership cargo arrangement

183



## 184 2.2 Computations

185

186 After the proper definition of the parametric model, several computations take place, in order to  
187 produce the required values, which are then used as input during the calculation of the performance  
188 indicators examined in the present study.

189

190 For this reason, custom features are created within the software. Cargo capacity is automatically  
191 computed thanks to a feature that retrieves information from those responsible for the creation of the  
192 cargo arrangements. Apart from the actual measurement of the TEUs below and above the main deck,  
193 these features are designed to calculate the vertical and longitudinal moments, as well as the vertical  
194 and longitudinal centres of gravity, which are used as input in other computations.

195

196 Before proceeding to the remaining computations, a hydrostatic calculation is run first. Earlier, the  
197 same action took place; however, it was before the final hull was generated. Since its characteristics  
198 have changed after the last hydrostatic computation, a new run is necessary for the following steps of  
199 the project.

200

201 Custom features estimate the total ship resistance ( $R_T$ ) according to the Holtrop and Mennen method  
202 (Holtrop & Mennen, 1978). Holtrop and Mennen method is one of the mostly used empirical methods  
203 to estimate the resistance and propulsion requirements. It is believed to produce satisfactory results.

204 The aim of this study is to find an optimal containership design using a fast optimisation procedure,  
205 hence CFD was not utilised in this case, although it would be preferred over an empirical method as  
206 more accurate results would be produced through CFD. Since the method is programmed within the  
207 core software tool, the calculations are done fast and an estimation of the total resistance of the hull is  
208 obtained without having to run time-consuming CFD analyses. The overall resistance is divided into  
209 categories as defined by the aforementioned method. At this stage, the service speed of our model is  
210 determined, since it is required for the calculations. Taking into account the recent trend of slow  
211 steaming, the operational speed is set to 20 knots.

212

213 The Holtrop and Mennen method includes formulas for the estimation of the effective horsepower  
214 (EHP) and the shaft horsepower (SHP) (Holtrop & Mennen, 1978). First, the EHP is calculated, since  
215 both the total resistance and the vessel's speed are known. Having already found the necessary  
216 propulsion and efficiency factors from the resistance computations, the calculation of SHP is then  
217 possible. The final result is increased by 20% to include a sea margin as well as the impact of hull  
218 fouling, representing the common practice in the shipping industry (MAN Diesel & Turbo, 2011).  
219 Next, the estimation of the auxiliary power follows. Finally, the fuel consumption is estimated. Next,  
220 the estimation of the auxiliary power follows, using the following formula:

221

$$P_{B_{Aux}} = 100 + 0.55 \cdot P_{B_{ME}}^{0.7}$$

222

223 The next step is to calculate the lightship of the modelled ship. The lightship weight is divided into  
224 three categories; the steel weight, outfitting weight, and the machinery weight. Steel weight is  
225 computed using the Schneekluth and Müller-Köster methods. Outfitting and machinery weights are  
226 calculated using existing formulas, taking as input several parameters, such as the main dimensions of  
227 the ship, as well as the main engine's power (Papanikolaou, 2014). In addition, longitudinal and  
228 vertical centres of gravity are estimated, to be used later at the generation of the examined loading  
229 cases.

230

231 Even though the methods utilised for this step are semi-empirical approaches, and thus, an  
232 approximation of the exact values, we aim at the most accurate results. In this context, it should be  
233 noted that several parameters needed for the computations are derived from applications and detailed  
234 calculations performed by the CAESES®, such as the enclosed volume of the hull, which is very  
235 important for the rest of the process. Moreover, the formulae were calibrated using a similar 6,300  
236 TEU containership, for which detailed lightship breakdown and other data were available. This  
237 allowed the calculation of correction factors that would improve the final outcome of the model's

238 lightship estimation, since the actual lightship weight and centre of gravity of the reference ship were  
239 known. Thus, first, all required calculations for the reference ship were performed in Microsoft  
240 Excel® (Microsoft, 2010) and a customised code was developed in CAESES®, including the methods  
241 used in the first step, so as to determine the model's lightship characteristics. It should be noted that  
242 this feature takes as input the data from the computations performed in Microsoft Excel®, so as to  
243 include the correction factors in the model's lightship computation.

244

245 Afterwards, custom features responsible for the deadweight analysis generate the necessary values for  
246 the determination of the loading cases examined. An operational profile is set up at this stage, so as to  
247 reckon the amount of consumables carried on board (Table 1).

248

249 Table 1: Operational profile

250	Operational speed (knots)	20
251	One-way route distance (nm)	12,205
252	Number of ports	18
253	Average time at port (h)	15.3
254	Transit time (days)	63

255

256 The final design computation that has to be performed is the allocation of the necessary tanks in the  
257 model's hull. The tanks created in the model are mainly the ones containing the fuel, diesel and lube  
258 oil, as well as the water ballast tanks. At first, sections which represent the tanks are generated. Then,  
259 hydrostatic calculations are performed to determine the basic properties of the tanks, such as the  
260 volume, weight, and their centre of gravity.

261

262 2.3 Performance indicators

263

264 Following the definition of the features responsible for the naval architectural computations, the  
265 development of those responsible for the determination of the design indicators takes place. These  
266 indicators will then be used as the objectives in the optimisation procedure.

267

268 One of the optimisation criteria in our project is the minimisation of the EEDI. A custom feature is  
269 programmed in order to calculate both the required and the attained EEDI values, according to the  
270 regulations (IMO, 2012c). The required EEDI value is calculated based on the following formula:

271

$$EEDI_{req} = a \times b^{-c} \times \left(1 - \frac{x}{100}\right)$$

272

273 Where a and c are equal to 174.22 and 0.201, respectively, according to the IMO in case of  
274 containerships, b stands for the deadweight of the vessel, and x is a reduction factor. The feature is  
275 programmed in such way to include the reduction factor as a parameter that can change within the  
276 creation of the model. In the present study, the optimisation is run for the current conditions, i.e. the  
277 reduction factor is considered to be equal to 10%. However, the designer can select the desired value,  
278 depending on the conditions that have to be met in a particular study.

279

280 On the other hand, the attained EEDI value is calculated using the following conceptual formula  
281 (measured in gr CO<sub>2</sub>/tonne mile):

282

$$EEDI_{att} = \frac{(\text{Ship emissions}) - (\text{Ship emissions reduction by efficiency technologies})}{(\text{Transport work})}$$

283

284 The ship emissions include that of the main engine, auxiliary engines, as well as the shaft generators,  
285 and motor emissions. The efficiency technologies include several arrangements, modifications, or  
286 installations to the hull or the propulsion system, which result in increased efficiency. Hence, these  
287 technologies should be taken into account in the calculation of the attained EEDI as a reduction factor.

288 Finally, the transport work takes into account the cargo loading of the ship, as well as its service speed  
289 (DNV GL, 2013, MAN Diesel & Turbo, 2015).

290

291 Apart from producing the values mentioned above, an “attained/required” EEDI ratio is also  
292 calculated, to be used as a constraint during the optimisation phase.

293

294 Another significant performance indicator for this study, the required freight rate (RFR), is also  
295 calculated by use of newly developed features in CAESES®. This value indicates the minimum rate  
296 that evens the properly discounted ship’s expenses. The main formula used to calculate the RFR is the  
297 following (Watson, 1998):

298

$$\text{RFR} = \sum_i^N \left[ \frac{\text{PW(Operating cost)} + \text{PW(Ship acquisition cost)}}{(\text{Round trips}) \times (\text{TEUs})} \right]$$

299

300 where PW is the present worth of the respective cost. The overall cost is divided into two categories;  
301 the operating cost and the ship acquisition cost. The former is mainly based on the running costs of  
302 the ship, such as cost for the fuel, crew, stores, maintenance, insurance, administration, and port costs.  
303 As far as the fuel cost is concerned, a review is made first, so as to identify the HFO and MDO costs.  
304 Then, taking into account the route length and the fuel consumption of the model, the total fuel cost is  
305 reckoned. As far as the ship acquisition cost is concerned, to perform the calculations, several data are  
306 used as input, including the steel mass of the vessel, cost of steel, discount rate, operation time, main  
307 dimensions, and engines’ power (Soulтанias, 2014).

308

309 One of the most important innovation elements in the model is the control of trim and stability, while  
310 optimising for maximum number of containers on deck and minimum carried ballast. This step is  
311 essential for the implementation of the next one, namely the generation of the loading cases. Within  
312 this software module, essential ship hydrostatic and stability parameters are determined, such as the  
313 values of the restoring arm lever GZ-φ curve, the trim of the ship, as well as the vertical centre of

314 mass KG and longitudinal centre of mass LCG values that are used in the loading cases computation.  
315 The stability is evaluated by assuming a homogenous stow. The assessment of the initial and large  
316 angle stability of the vessel is undertaken for common type loading conditions in accordance with the  
317 IMO A.749/A.167 intact stability criteria. The code used in this project generates the GZ- $\phi$  curve, by  
318 running several hydrostatic computations at various heeling angle values. A continuous check is  
319 performed, to ensure that the model complies with the IMO intact stability criteria. If the latter is not  
320 the case, the stowage of cargo, ballast and fuel, along with the associated KG and LCG values are  
321 modified and the whole process is repeated, until the criteria are met. The ultimate goal of this  
322 iterative procedure is to minimise the amount of carried water ballast and identify “zero ballast”  
323 loading conditions. During this procedure, the payload weight, calculated based on the homogenous  
324 weight per TEU, as well as its vertical centre of gravity are taken into account.

325

326 A new element introduced in this optimisation problem, compared to previous similar studies (Priftis  
327 et al., 2016b) is the consideration of the imminent changes in the stability regulations. In particular,  
328 the level 1 and 2 draft criteria for parametric roll failure mode according to the IMO are applied in this  
329 project (IMO, 2015). The level 1 criterion, based on the Mathieu equation, is meant to be simple and  
330 conservative, in order to quickly detect a vulnerability to parametric roll. On the contrary, level 2  
331 criterion is more complex and accurate, taking into account more detailed parameters so as to  
332 determine whether the ship is vulnerable to parametric roll or not. In order to properly define a way to  
333 perform the level 1 and 2 checks within CAESSES®, multiple features are created, each one having a  
334 specific purpose. Moreover, several external software programmes are connected with the model, so  
335 as to quickly evaluate certain parameters required for these particular computations. Maxsurf Stability  
336 Enterprise® (Bentley Systems, 2014) is used to produce values of the metacentric height (GM) in  
337 various wave conditions, as proposed by the regulations, while Matlab® (Mathworks, 2014) is  
338 responsible for the calculation of the roll amplitude during the level 2 criterion check, where complex  
339 equations must be solved.

340

341 The last computation required is the generation of the loading conditions. A custom feature was  
342 developed for this purpose. The loading conditions investigated in this study are the maximum TEU  
343 capacity and the “zero ballast” conditions. Both of them require several parameters and elements  
344 determined in previous stages. These parameters consist of various weight groups, as well as their  
345 longitudinal and vertical centres of gravity which represent the data used as input in this computation.  
346 These groups include the displacement, the lightship, the payload, divided into the below and above  
347 main deck TEUs, the consumables, and the water ballast. As far as the water ballast is concerned,  
348 several groups are defined, to fill only the minimum required space with sea water.

349

350 For the maximum TEU capacity case, the main objective is to maximise the cargo capacity. On the  
351 other hand, the “zero ballast” condition is defined as a condition where no water ballast is loaded for  
352 stability reasons, with the exception of some limited water ballast in the aft and fore peak tanks, for  
353 trim balance. As in the former case, the objective is the maximisation of the number of loaded TEUs.

354

355 Following the definition of the loading cases, two performance indicators are created; the port  
356 efficiency and the zero ballast water indicators. The former is represented by an “on deck/in hold”  
357 stowage ratio, which takes as input the number of containers stacked above and below the main deck,  
358 calculated in a previous computation. The objective is to maximise the ratio i.e. the number of TEUs  
359 stored on deck. As far as the zero ballast condition is concerned, a performance indicator, which is  
360 also one of the objectives of the optimisation procedure, is defined at this stage. Instead of using the  
361 actual TEU capacity of the zero ballast condition, a parameter representing a capacity ratio is used.  
362 This ratio is defined by dividing the number of containers the ship can transport while in zero ballast  
363 to the maximum TEU capacity of the ship. As in the case of stowage ratio, the higher the capacity  
364 ratio, the more competitive is the vessel.

365

366 2.4 Design exploration

367

368 Before proceeding to the formal optimisation round, a design of experiment (DoE) is conducted first.  
369 This process allows the examination of the design space and the response of several parameters to the  
370 change of the model's main characteristics. The algorithm utilised is the Sobol algorithm, a quasi-  
371 random sequence which secures the overall coverage of the design space, while overlapping of  
372 previous set of sequences is avoided (Mohd Azmin & Stobart, 2015). Through the DoE, the  
373 investigation of the feasibility boundaries is ultimately achieved, allowing the detection of the trends  
374 of the design variables (Table 2) with regard to the optimisation objectives. In our case, the design  
375 engine is assigned to create 250 variants of the initial model. At this point, no objectives need to be  
376 determined, since only the feasibility boundaries are investigated. However, several parameters are  
377 evaluated through this process.

378  
379 The design variables used in this study are presented in table 2. They consist of TEU arrangement  
380 elements, such as the number of bays and rows, certain hull dimensions, such as the double bottom, as  
381 well as the variation of the  $C_P$  and LCB values. Since the main dimensions of containerships are  
382 highly dependent on the container arrangement, the main dimensions of the model derive from these  
383 design variables. For instance, the beam of the hull is calculated by taking the number of rows, the  
384 beam of each container and the double side dimension into account. As far as the variation of the  $C_P$   
385 and LCB values are concerned, the range selected in this case represents the percentile change in the  
386 values used in the baseline model, in order to apply the Lackenby transformation on the hull to create  
387 a new variant.

388

389 Table 2: Design variables

390 Design variable	Minimum value	Maximum value
391 Bays	18	20
392 Rows	14	18
393 Tiers in hold	8	10
394 Tiers on deck	6	8
395 Double bottom (m)	2.00	3.00



396	Double side (m)	2.00	3.00
397	$\delta C_p$	-0.06	0.06
398	$\delta LCB$	-0.026	0.026
399	Bilge radius (m)	4	6

400

401 Moreover, the constraints are set (Table 3), so as to have a clear view of which of the subsequent  
402 variants violate criteria that must be met.

403

404 Table 3: Design constraints

405	Constraint	Value
406	“Attained/required” EEDI	$\leq 1$
407	GZ area (0-30 deg)	$\geq 0.055$ m-rad
408	GZ area (0-40 deg)	$\geq 0.09$ m-rad
409	GZ area (30-40 deg)	$\geq 0.03$ m-rad
410	Initial metacentric height GM	$\geq 0.15$ m
411	Angle at $GZ_{max}$	$\geq 30$ deg
412	$GZ_{max}$	$\geq 0.2$ m
413	Homo weight/TEU (maximum TEU capacity)	$\geq 6$ t
414	Homo weight/TEU (zero ballast condition)	$\geq 7$ t
415	Trim at full load departure condition	$\leq 0.5\%$ $L_{BP}$
416	Parametric roll criteria	$= 1$ (pass)

417

418 When the run ends, a wide variety of results are displayed, which provide information about the  
419 design space. It is worth mentioning that the TEU capacity of the model is not constrained, thus the  
420 maximum and minimum number of TEU capacity of the variants is not limited to the 6,000-7,000  
421 area.

422

423 2.5 Multi-objective optimisation

424

425 The last step to complete the procedure is to set up the formal optimisation round. To achieve that, the  
426 non-dominated sorting genetic algorithm II (NSGA-II) is utilised (Deb et al., 2002). In particular,  
427 during each run, 300 generations are created, having a population size of twelve, each. This results in  
428 a total of 3,600 produced variants. The design variable extents remain the same, as the design space  
429 proved to be well defined, following the DoE phase. In addition, the design variables' range remains  
430 the same, as the design space proved to be well defined. As far as the constraints are concerned, apart  
431 from the ones defined in the previous stage, two additional are set to delimit the maximum TEU  
432 capacity of the ship variants. Therefore, an upper (7,000 TEUs) and lower (6,000 TEUs) limit is  
433 defined. Unlike the previous phase, in this case, apart from the evaluation of various parameters of the  
434 model, several objectives are defined:

435

436 Minimisation of the RFR

437 Maximisation of the capacity ratio

438 Minimisation of the EEDI

439 Maximisation of the stowage ratio

440 Minimisation of the overall ship resistance

441

442 The results of a multi-disciplinary optimisation procedure define the Pareto front of the non-  
443 dominated designs. As the decision maker needs to select one design, Multi Attribute Decision  
444 Making (MADM) is applied. Several case scenarios are created, so as to determine the optimal of the  
445 top solutions to the problem. In this study, three distinctive scenarios are defined, where the  
446 significance of each objective is acknowledged differently by assigning specific "weights" following  
447 the utility functions technique of decision making theory (Table 4) (Sen & Yang, 1998). In scenario 1,  
448 all five objectives are considered to be equally important; hence each one is assigned a weight at  
449 saturation of 20%. On the other hand, in scenarios 2 and 3, the RFR and capacity ratio are chosen  
450 respectively to be more significant for the decision maker (designer, operator) by assigning to them a  
451 weight of 50% and 20% for the most important and the second most important objective in both cases,

452 whereas the rest are assigned a weight of 10%. After obtaining the results of each run, the data are  
453 normalised according to the scenarios. Next, the normalised data are ranked to find the optimal variant  
454 of our model. The maximum score that can be achieved after this process for each design, in each case  
455 scenario, is 1, whereas the lowest is 0. In most cases, a specific variant dominates in every scenario.

456

457 Table 4: Case scenarios

458 Objective	Scenario 1	Scenario 2	Scenario 3
459 RFR	20%	50%	20%
460 Capacity ratio	20%	20%	50%
461 EEDI	20%	10%	10%
462 Stowage ratio	20%	10%	10%
463 Ship resistance	20%	10%	10%

464

### 465 3 DISCUSSION OF RESULTS

466

#### 467 3.1 Base model

468

469 Before proceeding to the actual results, some essential information about the base model is presented,  
470 in order to have a clear perspective of the initial hull (Tables 5-6).

471

472 Table 5: Base model design variable values

473 Design variable	Base model value
474 Bays	19
475 Rows	16
476 Tiers in hold	9
477 Tiers on deck	6
478 Double bottom (m)	2.0
479 Double side (m)	2.1

480	$\delta C_p$	-0.01125
481	$\delta LCB$	-0.00375
482	Bilge radius (m)	5

483

484 Table 6: Base model design objective values

485	Objective	Base model value
486	RFR (\$/TEU)	582.35
487	Capacity ratio	0.5206
488	EEDI (gr CO <sub>2</sub> /tonne mile)	8.80
489	Stowage ratio	0.9451
490	Ship resistance (kN)	1,559

491

### 492 3.2 Design of experiment

493

494 The DoE phase enables the exploration of the huge design space, which is impossible in traditional  
 495 ship design procedures. The following observations can be made.

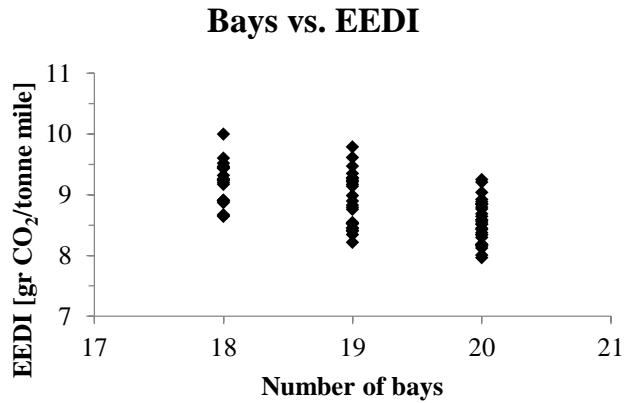
496

497 As far as the correlation between the number of bays and the attained EEDI is concerned, it is evident  
 498 that as the former increases, the latter decreases (Fig. 5). As the number of the bays gets higher, since  
 499 the total TEU capacity is not constant, the number of containers carried on board also rises, resulting  
 500 in a higher deadweight value. Since the latter is inversely proportional to the attained EEDI value, it  
 501 can be understood that there is a strong relation between the number of bays and the EEDI value.

502 Similar behaviour can be observed in the correlation between the number of rows and the attained

503 EEDI –the total TEU capacity is variable in this case as well (Fig. 6).

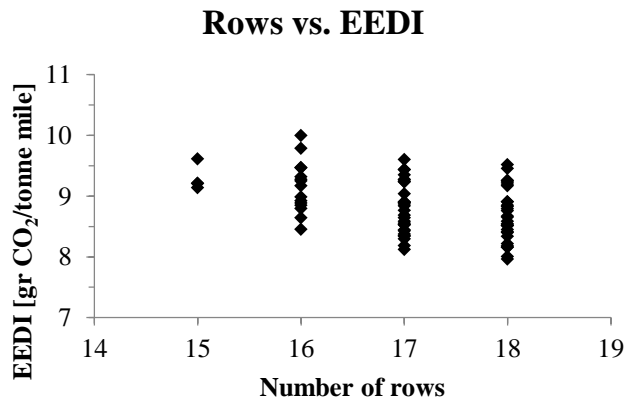
504



505

506 Figure 5: Bays vs. EEDI

507



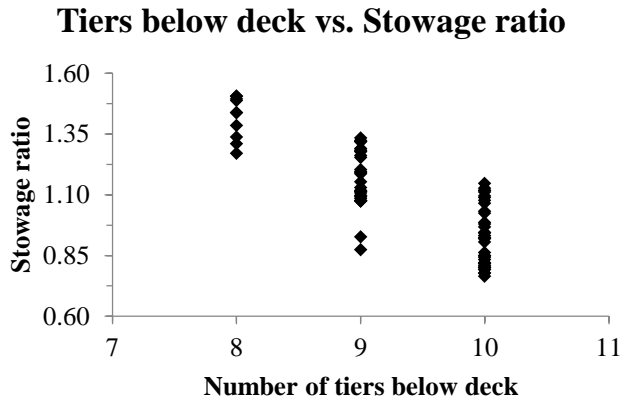
508

509 Figure 6: Rows vs. EEDI

510

511 Furthermore, the relation between the tiers below the main deck and the stowage ratio is presented in  
 512 figure 7. The higher the number of the container stacks, the lower the stowage ratio. This trend is  
 513 expected, as the increase in the number of TEUs below the main deck results in a lower number of  
 514 containers stacked above the main deck, for a given TEU capacity range.

515



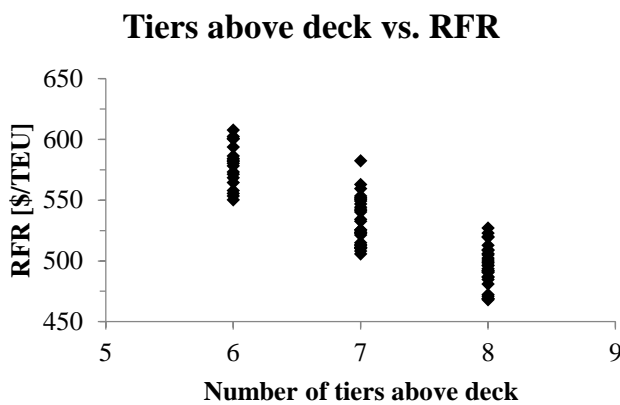
516

517 Figure 7: Tiers below deck vs. stowage ratio

518

519 Finally, as far as the dependency of the RFR on the number of tiers above the main deck is concerned,  
 520 it is evident that the RFR decreases, as the latter increases (Fig. 8). As previously mentioned the  
 521 number of tiers below and above the main deck is interdependent. Moreover, it can be understood that  
 522 a tier located above the main deck contains more TEUs than one below the main deck, due to the hull  
 523 shape restrictions. Hence, by increasing the number of tiers above the main deck, a larger cargo  
 524 capacity can be achieved for the same main dimensions of the ship, which in turn leads to a lower  
 525 RFR.

526



527

528 Figure 8: Tiers above deck vs. RFR

529

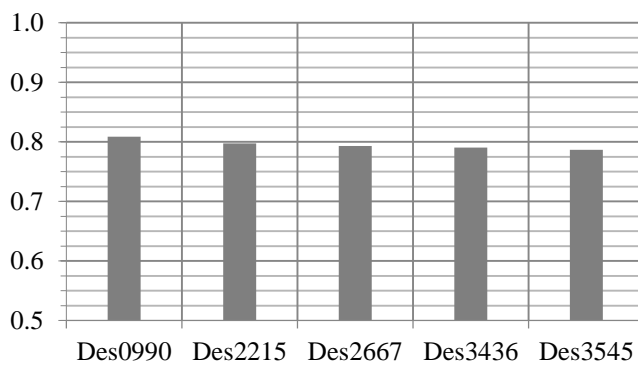
530 3.3 Multi-objective optimisation

531

532 Following the NSGA-II run and the evaluation of the results, an improved design, named Des0990, is  
533 identified. Des0990 ranked first in the first two case scenarios. A second variant, named Des0449,  
534 ranked first in the third scenario. Following the decision making process, Des0990 is ultimately  
535 selected as the optimal design (Figs. 9-11). Below, some principal information of the optimised design  
536 can be found (Fig. 12, Tables 7-8).

537

### Scenario 1

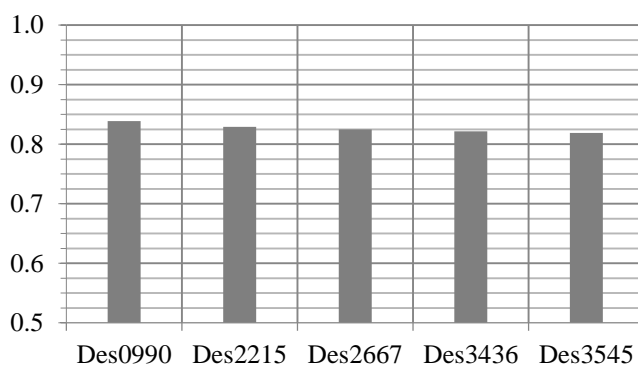


538

539 Figure 9: Scenario 1 ranking

540

### Scenario 2

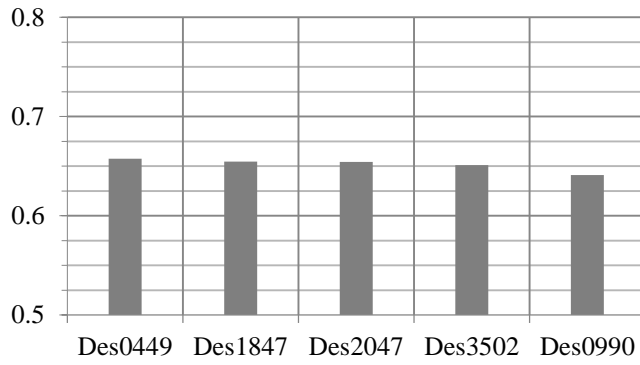


541

542 Figure 10: Scenario 2 ranking

543

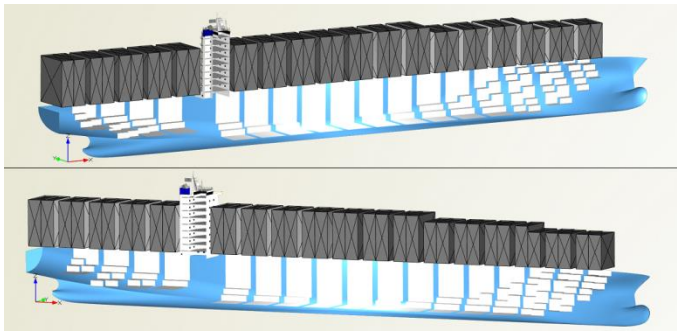
### Scenario 3



544

545 Figure 11: Scenario 3 ranking

546



547

548 Figure 12: Des0990 model

549

550 Table 7: Des0990 design variable values

Design variable	Des0990 value
Bays	19
Rows	15
Tiers in hold	8
Tiers on deck	8
Double bottom (m)	2.78
Double side (m)	2.07
$\delta C_p$	-0.05624
$\delta LCB$	0.02376
Bilge radius (m)	4.877

560



561

562 Table 8: Des0990 objective values

563 Objective	Des0990 value
564 RFR (\$/TEU)	501.55
565 Capacity ratio	0.5314
566 EEDI (gr CO <sub>2</sub> /tonne mile)	8.51
567 Stowage ratio	1.4553
568 Ship resistance (kN)	1,429

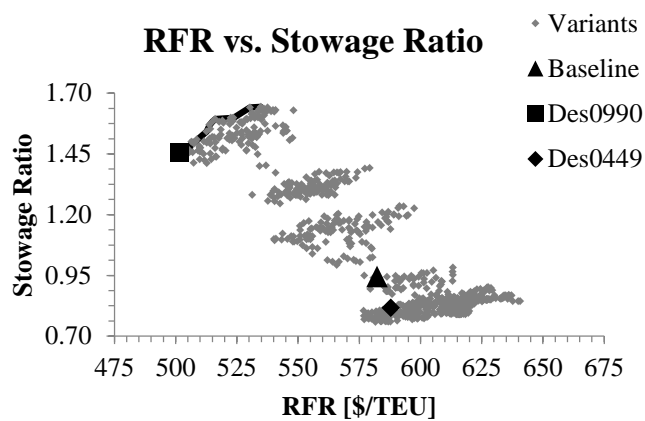
569

570 A set of graphs containing the relation between the optimisation objectives is presented below. The  
571 Pareto front is demonstrated by a solid black line in each case.

572

573 As far as the values of the RFR and the stowage ratio are concerned, a favourable trend can be  
574 observed. In particular, it can be understood that the higher the stowage ratio, the smaller the freight  
575 rate. As one would expect, as the stowage ratio rises, the total number of containers transported is  
576 increased for a given set of main dimensions. Hence, the deadweight is increased and the RFR value  
577 gets lower (Fig. 13).

578

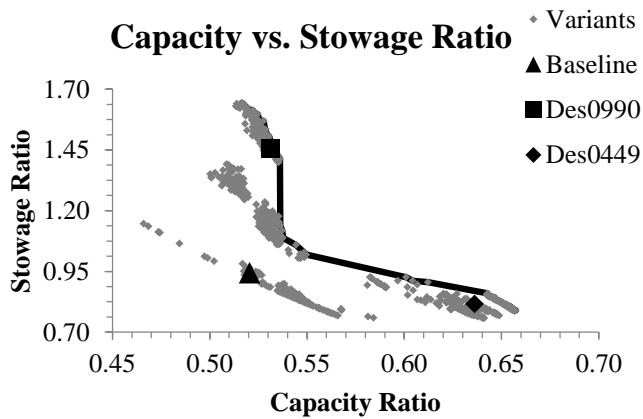


579

580 Figure 13: RFR vs. stowage ratio

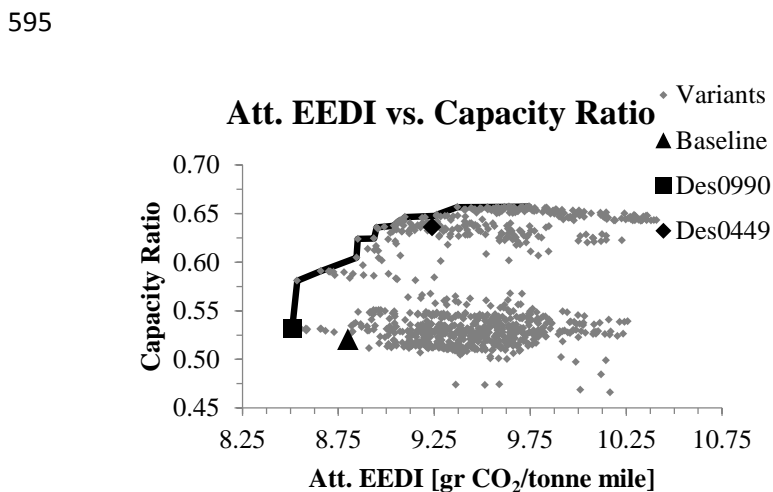
581

582 In case of the two examined ratios –capacity and stowage– an inversely proportional trend can be  
 583 observed. Variants which feature high stowage ratio are characterised by low capacity ratio and vice  
 584 versa. This is the main difference between the two identified designs, Des0990 and Des0449 (Fig. 14).  
 585



586  
 587 Figure 14: Capacity vs. stowage ratio

588  
 589 As far as the relationship between the attained EEDI and the capacity ratio is concerned, a clear  
 590 Pareto front can be identified. There are many designs in the range between 0.625 and 0.650 (as far as  
 591 the capacity ratio is concerned) that feature an attained EEDI value of 8.75 up to 10.50 gr CO<sub>2</sub>/tonne  
 592 mile. The identified improved design Des0990 has one of the lowest EEDI values but a relatively  
 593 small capacity ratio. Nevertheless, Des0990 performed better than the baseline ship in that respect  
 594 (Fig. 15).



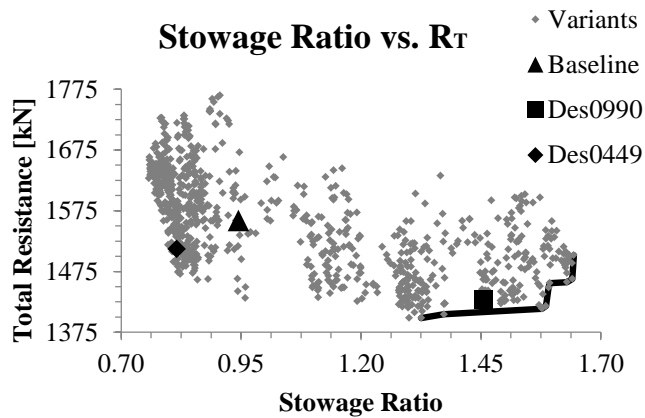
596

597 Figure 15: Att. EEDI vs. capacity ratio

598

599 Regarding the relation between the stowage ratio and the total resistance, a slight decline in the  
600 overall resistance can be observed, as the stowage ratio rises. Des0990 marks a great improvement as  
601 far as the stowage ratio is concerned, while it manages to achieve a lower total resistance (Fig. 16).

602



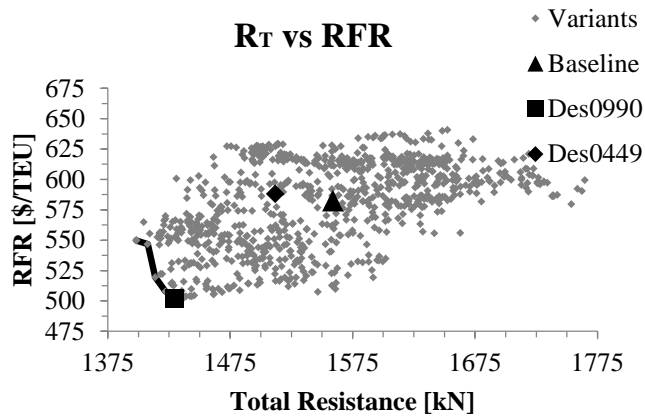
603

604 Figure 16: Stowage ratio vs. total resistance

605

606 Finally, it is worth commenting on the relation between then total resistance and the RFR. As in  
607 previous observations, it can be concluded that the resistance gets lower as the freight rate values  
608 become smaller (Fig. 17). Resistance influences directly the required power for propulsion. In  
609 addition, the fuel costs are taken into account in RFR estimation. Since fuel cost is proportional to the  
610 main engine's power, lower resistance means lower required power, which in turn can be translated to  
611 reduced fuel costs and lower RFR values.

612



613

614 Figure 17: Total resistance vs. RFR

615

616 The results presented above can be compared with previous optimisation runs on the same setup as  
 617 above (Priftis et al., 2016a). In particular, a less extensive NSGA-II run within CAESES® produced a  
 618 similar improved design, named Con156. During this run, 260 variants were created. Judging from the  
 619 graphs of these two optimisation results, similar Pareto fronts can be observed, which shows that  
 620 NSGA-II can get a uniform high-quality Pareto front in multi-objective optimisation problems with  
 621 excessive targeting. Details of the selected improved design produced during the less extensive  
 622 optimisation run can be found in tables 9-10:

623

624 Table 9: Con156 design variable values

625 Design variable	Con156 value
626 Bays	20
627 Rows	15
628 Tiers in hold	8
629 Tiers on deck	8
630 Double bottom (m)	2.50
631 Double side (m)	2.42
632 $\delta C_p$	-0.04662
633 $\delta LCB$	-0.01680

634 Bilge radius (m) 4.242

635

636 Table 10: Con156 objective values

637 Objective Con156 value

638 RFR (\$/TEU) 504.86

639 Capacity ratio 0.5233

640 EEDI (gr CO<sub>2</sub>/tonne mile) 9.04

641 Stowage ratio 1.5186

642 Ship resistance (kN) 1,496

643

644 Con156 features 20 bays, whereas Des0990 has one bay less than that. The number of rows and tiers  
645 above and below the main deck is the same in both cases. As far as the rest of the design variables are  
646 concerned, the differences are relatively small (Tables 7, 9). With regard to the objective values, a few  
647 similarities can be observed. For instance, both improved variants attained the best RFR values among  
648 the design variants in each run. In addition, both designs feature a relatively high stowage ratio;  
649 however, their capacity ratio is not one of the best that occurred during the optimisation runs. This can  
650 be explained by the fact that the stowage ratio has a greater impact in the optimal design selection  
651 during the MADM process. In both runs, the relation between the two ratios can be described as  
652 inversely proportional. Hence, a design with a high stowage ratio –and consequently a low capacity  
653 ratio value– was declared as the best among the produced variants in both cases. Finally, it should be  
654 mentioned that both Des0990 and Con156 achieved one of the lowest resistance values during the  
655 NSGA-II runs.

656

657 A one-to-one comparison between the baseline model and Des0990 is made, to show the percentage  
658 differences in several elements (Table 11).

659

660 Table 11: Baseline design vs. Des0990

661 Data Baseline Des0990 Difference

662	Bays	19	19	0
663	Rows	16	15	-1
664	Tiers in hold	9	8	-1
665	Tiers on deck	6	8	+2
666	Double bottom (m)	2.0	2.78	+0.78
667	Double side (m)	2.1	2.07	-0.03
668	Bilge radius (m)	5	4.877	-0.123
669	Total resistance (kN)	1,559	1,429	-8.33%
670	Maximum TEU capacity	6,487	6,789	+4.65%
671	Zero ballast TEU capacity	3,377	3,608	+6.84%
672	Capacity ratio	0.5206	0.5314	+2.07%
673	Stowage ratio	0.9451	1.4553	+53.98%
674	RFR (\$/TEU)	582.35	501.55	-13.87%
675	EEDI (gr CO <sub>2</sub> /tonne mile)	8.80	8.51	-3.29%

676

677 As far as the main dimensions are concerned, the improved design features the same amount of bays,  
678 while the number of rows and tiers below the main deck are decreased by one. Also, two extra tiers  
679 above the main deck are carried in the improved design. It should be noted that Des0990 is one of the  
680 few produced variants that feature eight tiers above the main deck. Due to stability restrictions, most  
681 of the successful design variants can carry only up to six or seven tiers of containers above the main  
682 deck. The extra tier found in Des0990 offers the advantage of an increased stowage and capacity ratio,  
683 as well as a reduced RFR, due to the higher total number of TEUs carried on board. In addition, the  
684 homogenous weight of each TEU in the maximum TEU capacity loading condition is 7.48 t, while in  
685 the zero ballast loading condition it is 22.15 t. Hence it is ensured that the containers will not collapse  
686 due to over-stacking, since the maximum number of tiers under and over the main deck is eight and  
687 the maximum superimposed load each ISO container can withstand is 192 t, according to regulations  
688 (IMO, 2014). Furthermore, the double bottom distance is higher in Des0990's case, while the double  
689 side distance and the bilge radius are reduced compared to the baseline design.

690

691 Overall, the improvement of the initial containership design is obvious. Des0990 manages to  
692 outperform the original in every objective. In addition, it should be noted that the attained/required  
693 EEDI ratio for the current state of the rules is equal to 0.53, providing a safety margin from the  
694 maximum allowed value set by regulations. On top of that, Des0990 manages to be a future-proof  
695 design, as the attained EEDI value of 8.51 gr CO<sub>2</sub>/tonne mile is in fact well below the value of 12.47  
696 gr CO<sub>2</sub>/tonne, which represents the reference line EEDI value when the reduction factor reaches the  
697 most conservative level of 30% in 2025 (Table 12). A notable improvement can be observed in the  
698 port efficiency factor and the RFR objectives, where an increase of 54% and a decrease of 14% are  
699 achieved, respectively.

700

701 Table 12: EEDI reference values

702 Design	Phase 1 (10%)	Phase 2 (20%)	Phase 3 (30%)
703 Baseline	15.87	14.10	12.34
704 Des0990	16.03	14.25	12.47
705 Des0449	16.11	14.32	12.53

706

707 4 SUMMARY AND CONCLUDING REMARKS

708

709 Through the work presented in this paper, the advantages of the utilisation of modern design  
710 optimisation in the shipbuilding industry have been demonstrated. By incorporating this type of  
711 parametric optimisation process in the early stages of ship design, a much improved design can be  
712 produced, providing numerous benefits to a potential builder and end user (ship owner). Furthermore,  
713 it is demonstrated that using modern CAD/CAE systems, it is possible to explore the huge design  
714 space with little effort, while generating excellent/partly innovative results within very short lead  
715 times. The presented methodology and the implemented CAD system allow the integration of more  
716 advanced tools for the improved modelling of e.g. ship's hydrodynamics or ship's strength. The  
717 optimisation can include other areas of ship design as main objectives, such as structural strength or

718 seakeeping, allowing naval architects to achieve a greater degree of holism in the design process  
719 (Papanikolaou, 2010).

720

721 It is evident that the relation of the design process with statutory regulations should be included in the  
722 optimisation process as well, as new rules are introduced every year. The present study incorporated  
723 new tools for the newly developed second generation criteria for parametric roll failure mode. The  
724 results indicate how the model should be designed to pass certain criteria to comply with international  
725 regulations, while it becomes clear that specific design parameters, such as the bilge radius and  
726 consequently, the midship coefficient, affect the above.

727

728 Compared to previous studies (Priftis et al., 2016b), the present paper shows that the consideration of  
729 newly developed intact stability criteria, such as the parametric roll check, influences the  
730 characteristics of the optimal containership design. Since these criteria have been recently developed,  
731 there are limited optimisation studies that take them into account. However, their consideration in a  
732 multi-objective design optimisation is important, as containership design will be affected once these  
733 criteria come into force. When parametric roll failure mode is not considered, an optimal  
734 containership would feature a different containership arrangement, compared to the optimal design  
735 identified in the present study. The introduction of new design parameters that extend the control over  
736 the hull increased the flexibility of altering the hull shape and led to new findings after the  
737 optimization was run. In addition, some parameters, such as the oil prices, differ between several  
738 optimisation studies, due to the fluctuation in prices throughout time and indicate that an optimal  
739 design can potentially be affected by such parameters. Future work could of course include the rest of  
740 the second generation intact stability criteria as part of the optimisation procedure, while uncertain  
741 parameters need to be treated accordingly to get more accurate results.

742

743 As far as the results of the current application are concerned, some general observations can be made  
744 and conclusions drawn.

745



746 The majority (71%) of the feasible variants produced during the optimisation process feature 15 rows.  
747 Since wider designs may be more prone to increased transverse accelerations in seaways, this  
748 observation seems to be valid, as the parametric rolling is taken into account in this optimisation  
749 study. The optimal design is characterised by the same number of row. Moreover, the highest ranked  
750 designs feature the minimum allowed number of tiers in hold. This can be explained by the fact that  
751 the maximisation of the stowage ratio is desired in this study. Hence, the number of TEUs below the  
752 main deck has to be minimal.

753

754 The methodology presented in this study can be also applied to other containership sizes or other ship  
755 types (Koutroukis et al., 2013, Soultanias, 2014). More phases of the ship's life cycle can be  
756 integrated to future studies, resulting in more comprehensive holistic ship design investigations  
757 (Papanikolaou, 2010).

758

## 759 5 ACKNOWLEDGEMENTS

760

761 This work was partially funded by the H2020 project "HOLISHIP-Holistic Optimisation of Ship  
762 Design and Operation for Life Cycle" (contract 689074).

763

764 The authors would like to express their sincere gratitude to the following people for their manifold  
765 support: Dr. Pierre Sames (DNV GL), Dr. Stefan Harries (Friendship Systems), Martin Köpke  
766 (HAPAG Lloyd, former GL), Timoleon Plessas (NTUA-SDL), George Koutroukis (former NTUA-  
767 SDL), Lampros Nikolopoulos (STARBULK, former NTUA-SDL), Ilias Soultanias (former NTUA-  
768 SDL), Aimilia Alisafaki (NTUA-SDL), Christos Gkerekos (UoS) and Sotirios Chouliaras (UoS).

769

## 770 6 REFERENCES

771

772 Abt, C. & Harries, S. 2007. Hull variation and improvement using the generalised Lackenby method  
773 of the FRIENDSHIP-Framework. *The Naval Architect*, 166-167.  
774 Bentley Systems 2014. *Maxsurf Stability*. Windows Version 20 ed.

775 Bonney, J. & Leach, P. T. 2010. Slow boat from China. *The Journal of Commerce*.

776 Brown, A. & Salcedo, J. 2003. Multiple-objective optimization in naval ship design. *Naval Engineers*  
777 *Journal*, 115, 49-62.

778 Campana, E. F., Liuzzi, G., Lucidi, S., Peri, D., Piccialli, V. & Pinto, A. 2009. New global  
779 optimization methods for ship design problems. *Optimization and Engineering*, 10, 533-555.

780 Deb, K., Pratap, A., Agarwal, S. & Meyarivan, T. 2002. A fast and elitist multiobjective genetic  
781 algorithm: NSGA-II. *IEEE Transactions on Evolutionary Computation*, 6, 182-197.

782 DNV GL 2013. Guidelines for determination of energy efficiency design index, rules for  
783 classification and construction, chapter VI: additional rules and guidelines, 13: energy  
784 efficiency. Hamburg, Germany.

785 Friendship Systems 2017. CAESES. 4.2.1 ed.

786 HOLISHIP 2016. Holistic optimisation of ship design and operation for life cycle. EU.

787 Holtrop, J. & Mennen, G. G. J. 1978. An approximate power prediction method. *International*  
788 *Shipbuilding Progress*, 25, 166-170.

789 IMO 1991. Navigation bridge visibility and functions. In: INTERNATIONAL MARITIME  
790 ORGANISATION (ed.). London, UK.

791 IMO 2004. BWM - international convention for the control and management of ships' ballast water  
792 and sediments. In: INTERNATIONAL MARITIME ORGANISATION (ed.). London, UK.

793 IMO 2012a. Consideration of the energy efficiency design index for new ships - minimum propulsion  
794 power to maintain the maneuverability in adverse conditions. In: INTERNATIONAL  
795 MARITIME ORGANISATION (ed.). London, UK.

796 IMO 2012b. Guidelines for calculation of reference lines for use with the energy efficiency design  
797 index (EEDI). In: INTERNATIONAL MARITIME ORGANISATION (ed.). London, UK.

798 IMO 2012c. Guidelines on the method of calculation of the attained energy efficiency design index  
799 (EEDI) for new ships. In: INTERNATIONAL MARITIME ORGANISATION (ed.). London,  
800 UK.

801 IMO 2014. IMO/ILO/UNECE Code of practice for packing of cargo transport units (CTU code). In:  
802 INTERNATIONAL MARITIME ORGANISATION (ed.). London, UK.

803 IMO 2015. Development of second generation intact stability criteria. In: INTERNATIONAL  
804 MARITIME ORGANISATION (ed.). London, UK.

805 IMO 2016. Marine environment protection committee. In: INTERNATIONAL MARITIME  
806 ORGANISATION (ed.). London, UK.

807 Köpke, M., Papanikolaou, A., Harries, S., Nikolopoulos, L. & Sames, P. 2014. CONTiOPT - holistic  
808 optimisation of a high efficiency and low emission containership. *Transport Research Arena*  
809 2014. Paris, France.

810 Koutroukis, G., Papanikolaou, A., Nikolopoulos, L., Sames, P. & Köpke, M. 2013. Multi-objective  
811 optimization of container ship design. 15th International Maritime Association of the  
812 Mediterranean - IMAM 2013. A Coruña, Spain: Taylor & Francis Group (CRC).

813 Kurt, I., Aymelek, M., Boulougouris, E. & Turan, O. 2015. A container transport network analysis  
814 study on the offshore port system case of west North America coast. *International Association*  
815 *of Maritime Economists - IAME 2015*. Kuala Lumpur, Malaysia.

816 Lackenby, H. 1950. On the systematic geometrical variation of ship forms. *Transactions of INA*, 92,  
817 289-316.

818 Maloni, M., Paul, J. A. & Gligor, D. M. 2013. Slow steaming impacts on ocean carriers and shippers.  
819 *Maritime Economics & Logistics*, 15, 151-171.

820 MAN Diesel & Turbo 2011. Basic principles of propulsion. Copenhagen, Denmark.

821 MAN Diesel & Turbo 2015. Energy efficiency design index. Augsburg, Germany.

822 Mathworks 2014. MATLAB. R2014a ed.

823 Microsoft 2010. Microsoft Excel.

824 Mizine, I. & Wintersteen, B. 2010. Multi-level hierarchical system approach in computerized ship  
825 design. 9th International Conference on Computer and IT Applications in the Maritime  
826 Industries - COMPIT 2010. Gubbio, Italy.

827 Mohd Azmin, F. & Stobart, R. 2015. Benefiting from Sobol sequences experiment design type for  
828 model-based calibration. *SAE Technical Papers*, 1.

829 Papanikolaou, A. 2010. Holistic ship design optimization. *Computer-Aided Design*, 42, 1028-1044.

- 830 Papanikolaou, A. 2014. Ship design: methodologies of preliminary design, Netherlands, Springer.
- 831 Peters, W., Belenky, V., Bassler, C., Spyrou, K. J., Umeda, N., Bulian, G. & Altmayer, B. 2011. The
- 832 second generation intact stability criteria: an overview of development. In: SNAME (ed.)
- 833 Annual Meeting of the Society of Naval Architects and Marine Engineers (SNAME).
- 834 Houston, Texas.
- 835 Priftis, A. 2015. Parametric design and multi-objective optimization of a 6,500 TEU container ship.
- 836 Diploma, National Technical University of Athens.
- 837 Priftis, A., Boulougouris, E., Turan, O. & Papanikolaou, A. 2016a. Parametric design and multi-
- 838 objective optimisation of containerships. International Conference on Maritime Safety and
- 839 Operations - MSO 2016. Glasgow, UK.
- 840 Priftis, A., Papanikolaou, A. & Plessas, T. 2016b. Parametric design and multiobjective optimization
- 841 of containerships. Journal of Ship Production and Design, 32, 1-14.
- 842 Sen, P. & Yang, J. B. 1998. Multiple criteria decision support in engineering design, London, UK,
- 843 Springer.
- 844 Ship & Bunker. 2017. Ship & bunker [Online]. Available: <http://shipandbunker.com/prices> [Accessed
- 845 September 2017].
- 846 Soultanias, I. 2014. Parametric ship design and holistic design optimisation of a 9K TEU container
- 847 carrier. Diploma, National Technical University of Athens.
- 848 Spyrou, K. J. 2005. Design criteria for parametric rolling. Oceanic Engineering International, 9, 11-
- 849 27.
- 850 Tozer, D. 2008. Container ship speed matters. London, UK: Lloyd's Register Group.
- 851 UNCTAD 2016. Review of maritime transport. Geneva, Switzerland.
- 852 van Marle, G. 2016. Intra-Asia beckons for panamax ships. Container Shipping & Trade. Enfield,
- 853 UK: Riviera Maritime Media Ltd.
- 854 Watson, D. G. M. 1998. Practical ship design, UK, Elsevier.
- 855 White, R. 2010. Ocean shipping lines cut speed to save fuel costs. Available:
- 856 <http://articles.latimes.com/2010/jul/31/business/la-fi-slow-sailing-20100731>.